THE ROYAL SOCIETY

Published online 29 December 2004

The motor mechanism of myosin V: insights for muscle contraction

H. Lee Sweeney[1] and Anne Houdusse[2*]

[1]*Department of Physiology, University of Pennsylvania School of Medicine, A700 Richards Building, 3700 Hamilton Walk, Philadelphia, PA 19104-6085, USA* (*isweeney@mail.med.upenn.edu*)

[2]*Structural Motility, Institut Curie CNRS, UMR144, 26 Rue d'Ulm, 75248 Paris Cedex 05, France* (*anne.houdusse@curie.fr*)

It is 50 years since the sliding of actin and myosin filaments was proposed as the basis of force generation and shortening in striated muscle. Although this is now generally accepted, the detailed molecular mechanism of how myosin uses adenosine triphosphate to generate force during its cyclic interaction with actin is only now being unravelled. New insights have come from the unconventional myosins, especially myosin V. Myosin V is kinetically tuned to allow movement on actin filaments as a single molecule, which has led to new kinetic, mechanical and structural data that have filled in missing pieces of the actomyosin–chemo-mechanical transduction puzzle.

Keywords: myosin; motility; unconventional myosin; X-ray structure; kinetics; chemo-mechanical transduction

1. INTRODUCTION

Fifty years ago, back-to-back publications in *Nature* by Hugh and Sir Andrew Huxley and their colleagues put forward the now accepted theory of muscle contraction; the sliding filament theory (Huxley & Hanson 1954; Huxley & Niedergerke 1954). In the years to follow, both Huxleys proposed models of how the myosin filaments used ATP to generate force and sliding of the actin filaments. Although the details of that mechanism are as yet unsettled, it would appear that elements of both the swinging cross-bridge of Hugh Huxley (1969) and the Brownian ratchet of Andrew Huxley (Huxley & Simmons 1971) may contribute to the contractile mechanism.

The ongoing discovery of non-filamentous myosins (so-called unconventional myosins, in contrast to the myosin II of muscle) that constitute the myosin superfamily began in 1973 (Pollard & Korn 1973). It has hastened the pace of elucidation of the contractile mechanism because within the superfamily are two-headed myosins that show processive movement (i.e. capable of multiple steps along the actin filament) as unloaded single molecules. Using one of these classes of myosins, myosin V, we have increased our insight into the kinetic, mechanical and structural properties of the motor, and at last are approaching a detailed understanding of its chemo-mechanical transduction.

2. ACTIN–MYOSIN ATPase CYCLE

That the sliding of the filaments was driven by consumption of ATP by the myosin itself was not demonstrated conclusively until 1962 (Cain & Davies 1962). Since then, kinetic studies have defined a myosin ATPase cycle that is catalysed by actin association and contains more states than have been seen in structural studies. The ATPase activity of myosin resides in its conserved motor domain, which is the major component of the cross-bridge that was observed to link the actin and myosin filaments in early EM photographs (Huxley 1957). The myosin motor domain interacts with actin, hydrolyses ATP, and produces the force necessary for movement along actin filaments. During the actomyosin ATPase cycle, weak actin-binding states (ATP and ADP-P_i states) alternate with strong actin-binding states (ADP states and nucleotide-free or rigour state). Biochemical, kinetic and mechanical studies on muscle myosins have established that ATP binding dissociates the actomyosin complex, and that ATP hydrolysis is rapid when myosin is not associated with actin. P_i release precedes ADP release and both product release steps are accelerated considerably upon actin binding. Force development occurs when myosin binds strongly to actin and is associated with actin-induced acceleration of P_i release.

The breakthrough in our understanding of the actin–myosin ATPase cycle came with the work of Lymn & Taylor (1971). Their transient kinetic analysis explained the puzzling observation that although myosin could only bind tightly to actin in the absence of ATP, actin greatly accelerated myosin's ATPase activity. Lymn and Taylor demonstrated that although myosin rapidly hydrolysed ATP in the absence of actin, rapid product release required a transient interaction with actin. Once the P_i and ADP have been released, ATP rapidly rebinds to the actin-bound myosin, causing rapid dissociation (Lymn & Taylor 1971).

From kinetic studies, it has been clear for some time that when myosin binds ATP, it must undergo a conformational change before it can hydrolyse ATP (Lymn & Taylor 1971). This structural transition was commonly denoted as

* Author for correspondence.

One contribution of 14 to a Discussion Meeting Issue 'Myosin, muscle and motility'.

a transition from M* to M** (two different fluorescent states of the myosin motor), which referred to its detection as a transition from a low to high tryptophan fluorescence state. (As discussed below, it is now clear that these two states have been visualized at high resolution and correspond to the structural states that we are now calling post-rigour (M*) and pre-powerstroke (M**).

Several studies also made clear that the M**·D·P (where D refers to ADP and P to inorganic phosphate P_i) state did not rapidly release P_i (now obvious in the pre-powerstroke state structures; see below) and thus following rebinding to actin in that state, a new state that allows P_i release must be induced by actin (Houdusse & Sweeney 2001). We speculate that this state may correspond to a state originally described by Sleep & Hutton (1980). Further, it is likely, but unproved, that this state can bind more strongly to actin than the pre-powerstroke state. The existence of such a state would be consistent with muscle fibre data (Dantzig *et al.* 1992). Following release of P_i, a strong actin-binding, strong ADP-binding state ($A.M.D^S$) is formed, but not populated for fast skeletal myosin II, at least in the absence of strain. This state is followed by a strong actin-binding, weak ADP-binding state ($A.M.D^W$) (Rosenfeld *et al.* 2000), from which ADP is released to form the rigour complex. All of these states are summarized in figure 3, in which only the kinetic states that are found in the predominant steady-state pathway are represented.

3. TWO HIGH-RESOLUTION STRUCTURES REVEAL AN ADENOSINE-TRIPHOSPHATE-DRIVEN SWITCH

The next major advance in the myosin field was the solving of the first high-resolution X-ray structure of myosin (Rayment *et al.* 1993*a*). The structure was of the entire S1 fragment (head) of chicken fast skeletal myosin. Although two and a half decades of biochemistry had given a general picture of what to expect, many of the details were unanticipated. Two key features of the structure generated immediate predictions about the myosin mechanism. First was the presence of a large cleft (see figure 1) in the middle of the head, which ran from the nucleotide-binding site to the actin interface (identified as such on the basis of earlier cross-linking studies). Rayment *et al.* (1993*a*) suggested that this cleft probably closes when myosin loses its hydrolysis products upon strong binding to actin. (Indirect evidence from EM combined with image reconstruction, as well as fluorescent probes located in the cleft, supported this prediction (Yengo *et al.* 1999; Volkman *et al.* 2000).)

The second striking feature and prediction of the Rayment structure focused on the myosin light chains. The light chains (which are members of the calmodulin superfamily) were bound to the C-terminal portion of the heavy chain, which formed an extended alpha helix. It appeared that in essence, this elongated domain formed a lever arm that could amplify small movements within the rest of the head (which Rayment *et al.* (1993*a*), referred to as the motor domain). This has come to be known as the lever arm hypothesis (Holmes 1996; Uyeda *et al.* 1996; Geeves & Holmes 1999; figure 2). This refinement of the swinging cross-bridge of Hugh Huxley (1969) proposes that relatively small motor domain rearrangements that are driven by actin binding and product release are amplified to induce a large swing of the lever arm during force

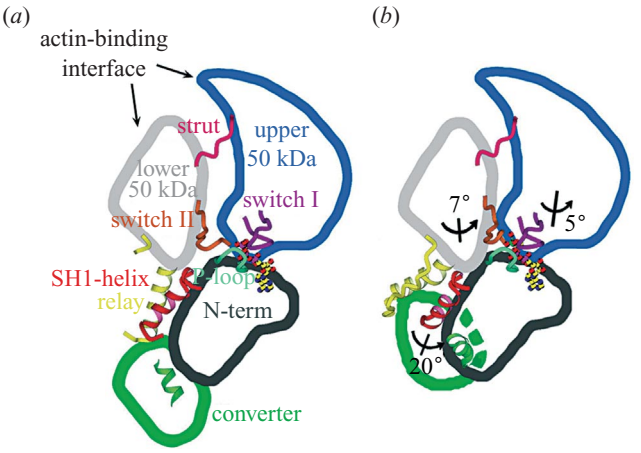

Figure 1. High-resolution structure of the myosin head in two different nucleotide states: (*a*) post-rigour (Mg^{2+}-ATP) and (*b*) pre-powerstroke (Mg^{2+}-ADP·P_i). A comparison of the motor domains of myosin in the first two high-resolution structural states showing the subdomain composition with associated connectors. The connectors and subdomains are coloured the same throughout and are labelled on (*a*). The structures have been positioned by superimposing the N-terminal subdomains. Relative to this subdomain, the amount of rotation necessary to move from the pre-powerstroke state to the post-rigour state is indicated on the subdomains of the pre-powerstroke state structure. Also indicated are the conformational changes in the four connectors (strut, switch II, relay and SH1 helix), as well as the positions of the nucleotide-binding elements, switch I and P loop. Note the large rotation of the converter domain to which the lever arm is attached (see figure 2).

generation. The second structural state of the motor described from crystal structures of myosin II with ADP·P_i analogues trapped (Fisher *et al.* 1995; Dominguez *et al.* 1998; Houdusse *et al.* 2000; Kollmar *et al.* 2002) supported this concept and allowed a high-resolution description of the state that hydrolyses ATP. In this state, the lever arm is in a pre-powerstroke or 'primed' position (Holmes 1996). By contrast, the lever arm is in a down position in structures with ADP or ATP analogues bound. This lever arm position is similar to that found for the final rigour state on actin (see figure 2), hence it has been referred to as the near-rigour state. We now are calling this state the 'post-rigour state'. (Note that while the original Rayment structure did not contain nucleotide, it did contain sulphate and was in the post-rigour conformation.) However, while the lever arm is in a position similar to rigour, the motor domain itself is in a very different state than in rigour, and indeed cannot bind strongly to actin. As described below, the unusual kinetics of myosin V provided an opportunity to view the structural changes that occur on actin, without having to bind myosin V to actin.

The nomenclature associated with the high-resolution structures is somewhat confusing. The name 'post-rigour' state is being used for the M* state, because it is the state that is formed when ATP attaches to the actomyosin rigour complex and dissociates the myosin from actin. It previously has been referred to as near-rigour, because the lever arm position is similar to that found in cryoEM actomyosin rigour complexes. It has also been called the open state, because of the switch II position. The pre-powerstroke state

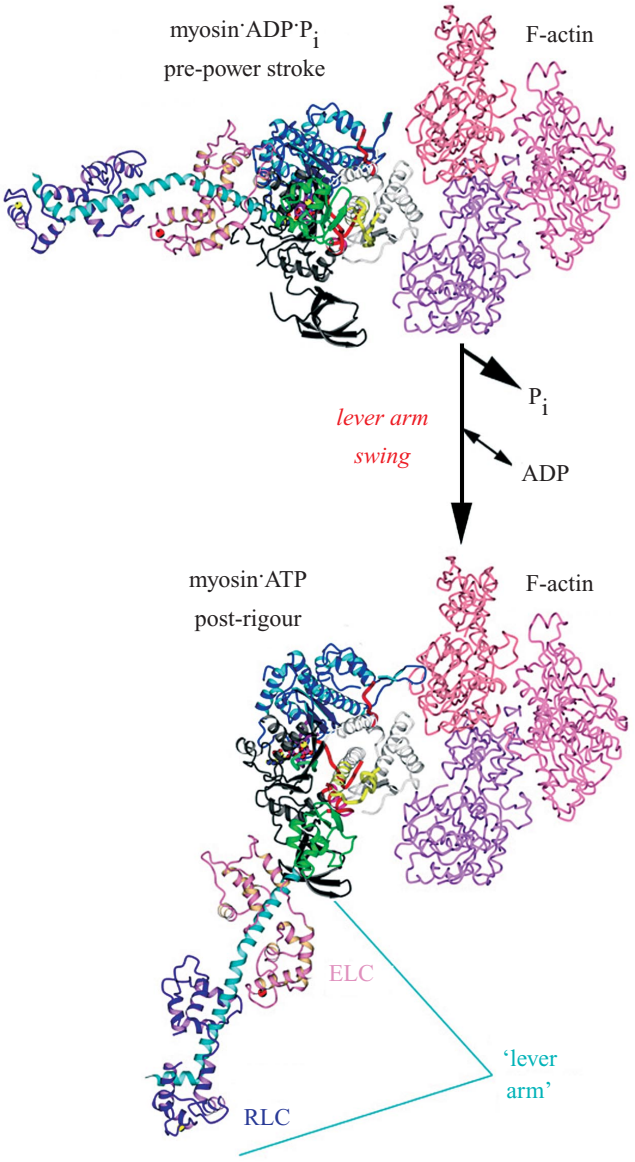

Figure 2. Structural basis for the myosin lever arm hypothesis. The first two high-resolution myosin structures (post-rigour and pre-powerstroke) suggested the adjacent scheme for actomyosin movement, which was termed the lever arm hypothesis. However, neither state binds strongly to actin, and this cannot be the true basis of force generation. While the pre-powerstroke state probably does represent the beginning of the powerstroke, the post-rigour state is not the end, but represents the state that ATP induces to detach myosin from actin.

(M**) is the post hydrolysis state (ADP·P$_i$) that binds to actin with the lever arm in a position that represents the beginning of the powerstroke. It has also been referred to as the transition state, because the initial AlFx structure was thought to be a transition state analogue. It has also been called the closed state, referring to the switch II position. We are referring to the high-resolution myosin V structure in the absence of nucleotide, which may closely represent the myosin conformation when bound to actin in the absence of nucleotide (rigour), as the rigour-like state.

Comparison of these structures shows that the myosin motor domain is functionally made up of four major subdomains that are linked by four deformable structural connectors (so-called 'joints') that are highly conserved in sequence (Houdusse *et al.* 1999; figure 1). These connectors are found at the periphery of the subdomains and can readily change conformation, in coordination with the movement of the subdomains relative to one another. Among these subdomains, the converter (which leads directly to the lever arm) has by far the greatest potential for movement because it is connected to the lower 50 kDa and N-terminal subdomains by only two deformable connectors (the relay and the SH1 helix). Rotation of the converter and lever arm can thus amplify relatively small conformational changes of the motor domain. Internal coupled rearrangements of the subdomains allow direct communication between the nucleotide-binding site, the actin binding interface and the lever arm. Coupling between the actin and nucleotide-binding sites is mediated via the large cleft between the upper and lower 50 kDa subdomains, which separates the actin-binding site in two distinct subdomains and communicates with the γ-phosphate pocket via a third connector, called switch II (see figure 1).

4. ACTIN–MYOSIN COMPLEX AND THE SWINGING LEVER ARM HYPOTHESIS

Fundamental requirements for understanding the mechanism of motility of myosin motors are detailed descriptions of the conformational changes within the motor, but also of the way in which the myosin motor interacts with the actin filament in different biochemical states. Structural insights into actomyosin interactions are largely derived from actin decorated filaments viewed with EM (Rayment *et al.* 1993*b*; Schröder *et al.* 1993; Whitaker *et al.* 1995; Jontes *et al.* 1995, 1998; Carragher *et al.* 1998; Volkman *et al.* 2000). The availability of high-resolution structures of an actin monomer (Kabsch *et al.* 1990; Otterbein *et al.* 2001), as well as models for the F-actin filament (Holmes *et al.* 1990 ; Lorenz *et al.* 1993) allowed the docking of atomic models into cryoEM maps to describe the contacts between actin and myosin in the rigour state. To interpret the myosin density, the post-rigour structures of myosin (ATP state) have been used because the lever arm adopts a down position in this state that is similar to that of myosin bound to actin in rigour (Rayment *et al.* 1993*b*). However, it is clear that the subdomains of the motor bound to actin are not in the same position in rigour and post-rigour structures, and that the rigour maps are best fit by a relative movement of the upper and lower 50 kDa subdomains towards each other (Rayment *et al.* 1993*b*; Holmes *et al.* 2003). (Compare the docking of post-rigour in figure 2 with the docking of rigour in figure 8. More detail is given in the contribution to this issue by Holmes *et al.* (2004).) This movement is necessary to generate a strong binding interface with actin, as myosin in the post-rigour conformation binds weakly to actin. It corresponds to the ATP-state of the motor that detaches from actin at the end of the cross-bridge cycle. Only the recently published myosin V nucleotide-free structure has a closed cleft (Coureux *et al.* 2003) necessary for strong actin binding, and thus it fits even the myosin II cryoEM maps better than the myosin II post-rigour structures (Holmes *et al.* 2004).

A second feature revealed by the EM structures is that for most myosins, there is a state where the lever arm is in an intermediate (between the pre-powerstroke and rigour)

position, and in which the myosin binds strongly to both actin and to ADP (Whitaker *et al.* 1995; figure 3). This intermediate actomyosin ADP state exists for the non-muscle, smooth muscle and cardiac muscle myosin IIs. Such a state in which both actin and ADP bind strongly is necessary to produce a highly strain-dependent ADP release step (Cremo & Geeves 1998; Nyitrai & Geeves 2004). Other muscle myosins, such as fast skeletal muscle myosin II, have weak affinities for ADP when bound to actin. They do not populate this intermediate state in the absence of load and the lever arm position in the rigour state is most similar to that of the strong ADP state of smooth muscle myosin II (Gollub *et al.* 1996; Rosenfeld *et al.* 2000; Volkman *et al.* 2003). This is probably an adaptation for speed of shortening, as it creates less strain dependence in the ADP release step, because less movement of the lever arm is required to release ADP.

The cryoEM observation of a swing of the lever arm upon ADP release for some myosins also gave indirect support for the swinging lever arm hypothesis of force generation. This hypothesis, summarized in figure 2, was originally postulated based on the fitting of atomic models of actin and myosin into observed actin and myosin rigour densities derived from cryoEM (Holmes 1996). In essence, the post-rigour state (ATP state) of myosin was equated with the end of the force generating cycle (powerstroke) of myosin and the pre-powerstroke state (taken to represent an ADP·P_i state) structure was proposed to represent the state before force generation. From the docking on actin, a $\sim$100 Å displacement of the myosin II lever arm towards the barbed end of the actin filament was predicted during the powerstroke (Holmes 1996).

Further experimental support for the swinging lever arm hypothesis comes from studies that show that the unitary displacement and/or velocity of myosin II are related to lever arm length (Uyeda *et al.* 1996; Warshaw *et al.* 2000; Manstein 2004). In particular, three reports demonstrated a direct correlation between lever arm length and stroke size (the displacement of a single-headed interaction with actin) of myosin V (Purcell *et al.* 2002; Sakamoto *et al.* 2003; Moore *et al.* 2004). Because the step size (the distance between actin subunits sequentially encountered by a two-headed molecule) of myosin V is bigger than the stroke size, these studies also show that a diffusive component contributes to the myosin V step size. Note also that although these studies support a role for swinging of the lever arm in the generation of force and movement, they do not address whether or not force production is directly coupled to lever arm movement.

5. DUTY RATIO

While all forms of myosin have the same kinetic cycle pictured in figure 3, the rates of transition between the states are highly variable. This allows myosin to be 'kinetically tuned' for a variety of cellular functions by not only altering the rate that it proceeds through the ATPase cycle, but also by changing the relative amount of the cycle that myosin spend in the strongly actin bound (force generating) states. The ratio of the occupancy of the strong states to the occupancy of the weak + dissociated + strong states is known as the duty ratio. Fast skeletal muscle myosin functions in large ensembles within the half sarcomere. Thus to maximize speed of shortening and power output, this type of myosin has a low duty ratio in the absence of load (i.e. the cross-bridges spend most of the cycle detached or weakly attached). Rapid detachment from the strongly bound states prevents drag on moving cross-bridges. Although more rapid detachment leads to higher shortening velocities, it also causes the isometric economy to be low. Thus, the smooth muscle and non-muscle myosins II have higher duty ratios and slower speeds of movement than skeletal muscle myosin II (Nyitrai & Geeves 2004).

6. MYOSIN V STEP SIZE AND PROCESSIVITY

The highest duty ratio myosins are those myosins that are capable of moving their cargo as a single molecule (De La Cruz *et al.* 1999). The ability of a single molecule to undergo multiple interactions with actin without releasing from the actin has been termed processivity. The first example of a processive myosin was myosin V (Mehta *et al.* 1999). Each head has a duty ratio that approaches unity at high actin concentrations. This ensures that when one head detaches from actin upon ATP rebinding, the other head will be in a strong binding state, and remain in a strong binding state long enough for the detached head to hydrolyse the ATP and rebind to a more distal actin binding site. In this manner myosin V can 'walk' along an actin filament. This property has made it possible to do mechanical studies on single molecules that have critically tested the lever arm hypothesis. Furthermore, the coordination between the heads of a single molecule that optimizes processive motion has led to new insights that are likely relevant for all myosins.

Image averaging of negatively stained myosin V molecules on actin filaments provided direct visualization of the two heads bound strongly to actin monomers that were separated by 36 nm (Walker *et al.* 2000). The lever arms of the two heads were in very different conformations. The images were interpreted as the lead head being in a pre-powerstroke conformation while the rear head was post-powerstroke (Burgess *et al.* 2002). Kinetic experiments recently published (Rosenfeld & Sweeney (2004) described below) make it clear that both heads of myosin V should have lost their P_i, indicating that the lead head must be in one of the states that follows the pre-powerstroke conformation. What is of great interest in visualizing such molecules is to relate the kinetic state of the lead head with the geometry of the lever arm, so as to understand how the internal strain is distributed to either deform the lever arm or distort elements within the motor domain itself.

Optical trap studies have also measured the step size and stroke size of a double-headed myosin V and have shown that there are preferred myosin binding positions (target zones) every 36 nm along the actin filament (Veigel *et al.* 2002). The 36 nm steps of the double-headed motor are a combination of the working stroke (21 nm) of the bound head and a biased, thermally driven diffusive movement (15 nm) of the free head onto the next target zone (Purcell *et al.* 2002; Veigel *et al.* 2002; Batters *et al.* 2004).

As mentioned above, a series of papers (Purcell *et al.* 2002; Sakamoto *et al.* 2003; Moore *et al.* 2004) demonstrated that both the stroke size of the single-headed constructs and the step size of the double-headed constructs

are linearly related to myosin V lever arm length. Later studies reinforced the lever arm role in myosin V, and provided evidence that it 'walks' in a hand-over-hand fashion along an actin filament (Yildiz *et al.* 2003), tilting its light chain binding domains as it does (Forkey *et al.* 2003).

7. KINETIC EXPERIMENTS WITH MYOSIN V

Before single molecule demonstrations of processivity, kinetic experiments on single-headed myosin V revealed that it achieves its high duty ratio in the absence of strain by having slow ADP release and fast ATP hydrolysis and P_i release. This leads to the predominant steady-state intermediate being a strongly bound actomyosin ADP state to which ADP is tightly bound. Myosin V, like smooth muscle myosin II, undergoes a lever arm swing (*ca*. 10° for myosin V) associated with ADP release. This provides a means of accelerating ADP release from the rear head, if the lead head pulls, and/or preventing ADP release from a lead head until the rear head detaches. These potential mechanisms of gating the heads to optimize processivity were recently addressed in kinetic experiments on double-headed myosin V constructs, as discussed below.

In collaboration with Steve Rosenfeld, we have performed kinetic experiments on the initial encounter of two-headed myosin V with an actin filament. This has allowed further insight into the kinetic scheme of myosin V (figure 3) that we initially described for a single-headed construct (De La Cruz *et al.*1999). The two-headed kinetic experiments, as well as recent trap experiments from the Spudich laboratory (T. J. Purcell, J. A. Spudich and H. L. Sweeney, unpublished data), have helped define the gating mechanism (as shown in figure 4) necessary for myosin V processivity.

The kinetic characterization is more complete for myosin V than for any other myosin. The reason that this is the case is that beginning with the release of P_i from AM·ADP·P_i, each actin-bound transition is more rapid than the one that follows it. For myosins in which slow steps precede fast steps, the two steps cannot be easily detected as distinct. For myosin V, the release of P_i is $\sim 200\ s^{-1}$ at 20 °C. (For the initial encounter of two-headed myosin V, both heads simultaneously release P_i at this rate.) This is followed by an isomerization of ADP states (weak to strong transition) that is detected by quenching of the pyrene actin signal and occurs at $\sim 25\ s^{-1}$ in the absence of strain at 20 °C. We refer to the initial ADP state (from which P_i is released) as the Sleep state, because it probably corresponds to the myosin II AM·ADP state described in muscle by Sleep & Hutton (1980). The transition from the Sleep state to the next state creates a strong ADP-binding, strong actin-binding state. This state has been observed by cryoEM for several myosins (Whitaker *et al.* 1995; Jontes *et al.* 1995). The rate of this isomerization appears to have a large temperature dependence, as the rate is at least four times faster at 25 °C than at 20 °C (De La Cruz *et al.*1999). This temperature sensitivity probably reflects a major structural rearrangement in the motor that is necessary to create a strong actin-binding interface. At 20 °C, the pyrene–actin quenching transition (weak to strong transition) is only slightly faster ($25\ s^{-1}$) than the isomerization that follows it in the cycle, which generates the state from which ADP is rapidly released. This isomerization rate is 13–15 s^{-1}. It is the step in the cycle that De La Cruz *et al.* identified as the overall rate-limiting step at 25 °C. The strong ADP-binding, strong actin-binding myosin V state is thus the predominate steady state intermediate in the cycle.

Rosenfeld & Sweeney (2004) measured the pyrene–actin quenching during steady-state turnover by a two-headed myosin V (before the onset of actin-cross-linking, so that both heads were bound to the same filament). The data were consistent with all rear heads being in a strongly bound state, and about half of the lead heads had released P_i, but had bound in a state that do not quench pyrene (Sleep state) and half that released P_i and bound in a strong, pyrene quenching, actin-binding state. This is what would be expected if the lead head does not accelerate ADP release of the rear head and the rear head does not markedly slow the weak to strong transition of the lead head (i.e. rear head releases ADP at 13 s^{-1} while the lead head simultaneously undergoes the weak to strong transition at 25 s^{-1}). Furthermore, the ADP release rate following the initial step was the same as the unstrained ADP release rate from a single-headed myosin V construct. Thus, these results imply that gating of two-headed myosin V is achieved by preventing the ADP-releasing isomerization of the lead head, rather than accelerating the ADP-releasing isomerization of the rear head.

Different results were obtained for the kinetics of the first actin encounter of the two-headed myosin V, than for the steady state. In that case, the two heads simultaneously bound to actin in the ADP·P_i state, simultaneously released P_i (200 s^{-1}), and simultaneously underwent an accelerated weak to strong transition (44 s^{-1}) at 20 °C. At that point, ADP release from the rear head was accelerated (30 s^{-1}), while ADP release from the lead head was prevented (gated) until the rear head detached. If the rear head was prevented from detaching (presence of high ADP/ATP), then dissociation of ADP from the lead head was at a rate of 0.3 s^{-1}. (This rate corresponds to the measured rate of ADP dissociation from the strong ADP-binding, strong actin-binding state of non-muscle myosin IIB (Rosenfeld *et al.* 2003).) As noted above, during the steps following the first step, no acceleration of ADP release was observed from the rear head, although ADP release was prevented in the lead head until the rear head detached. This difference in the ADP release rates from the rear head implies that the geometry of the initial encounter is different from subsequent encounters. This is reasonable because both heads are in an ADP·P_i state before the initial encounter, while only the lead head is in that state during the subsequent steps.

A somewhat different conclusion from the kinetic experiments of Rosenfeld & Sweeney (2004) was reached in optical trap studies from Veigel *et al.* (2002) who reported an approximately 1.5-fold acceleration of ADP release from the rear head by a lead head during processive stepping of myosin V. However, this assertion was based on comparisons of single encounters of two-headed myosin V molecules with encounters during processive runs. What was observed was that the duration of the event before ADP release was $\sim$ 107 ms in the single encounter case, versus 67–75 ms in the processive run. Thus, it would appear that ADP release from the rear head was faster during processive movement than during a single-headed

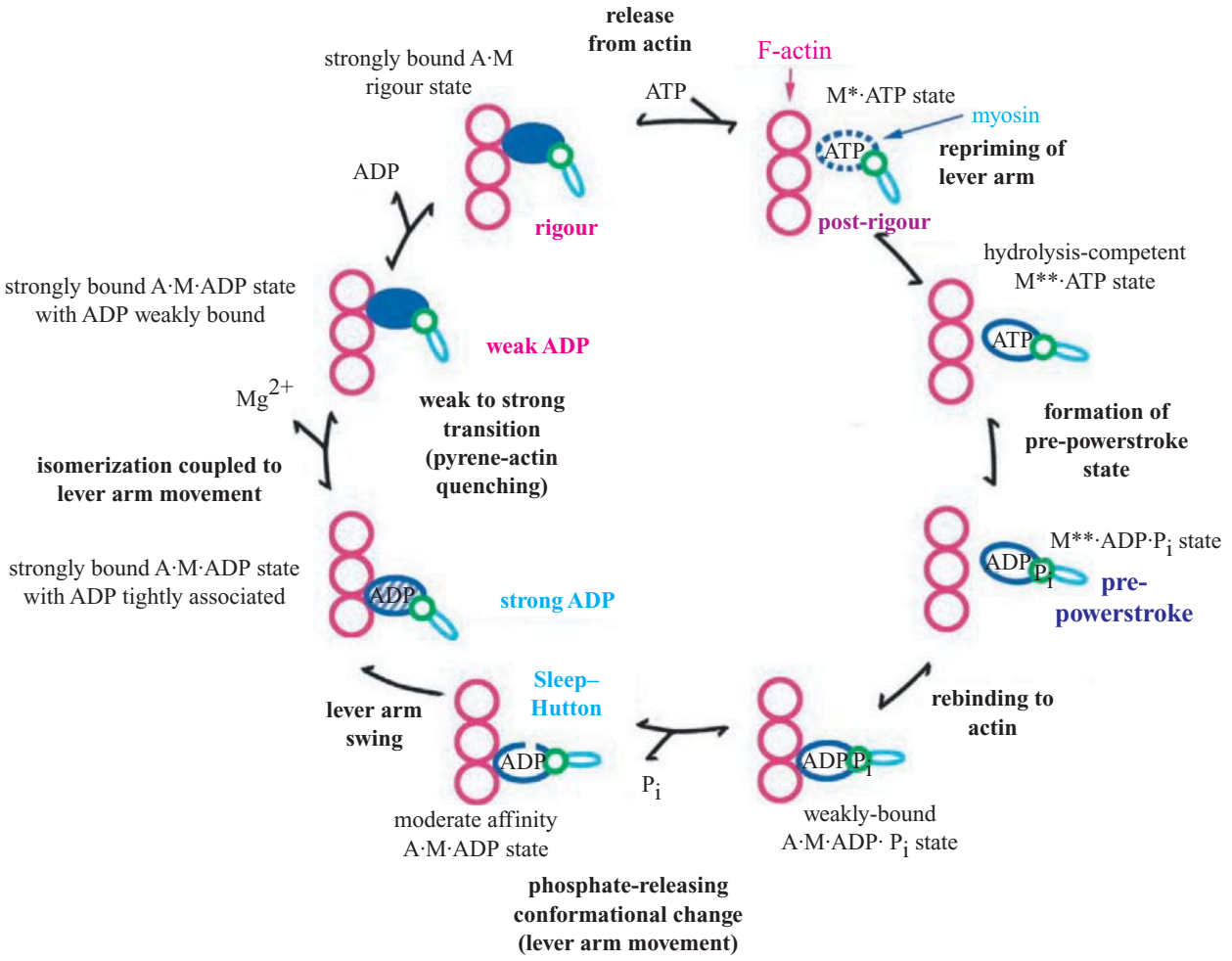

Figure 3. Actomyosin V ATPase cycle. This probably is a general kinetic scheme for all myosin family members. The major differences between myosins are the rates of P_i and ADP release, which ultimately determine the duty ratio. Another difference is that the strong ADP state either does not exist or is not populated in the absence of strain for a number of myosin isoforms, including vertebrate fast skeletal myosin II and *Dictyostelium* myosin II. We show release of Mg^{2+} occurring during the isomerization that creates the state from which ADP is rapidly released. We base this on a recent myosin V structure (P. D. Coureux *et al.* 2004), as well as the fact that high [Mg^{2+}] slows both the ATPase activity and motility of myosin V. We have labeled the affinity of the 'Sleep' state for actin as moderate (probably less than 1 μM), but no direct measurement of its affinity exists.

encounter. However, in light of the two-headed kinetic experiments of Rosenfeld & Sweeney (2004), this probably is a misinterpretation of the data. First, note that the 'accelerated' rate giving rise to the 67–75 ms duration corresponds to an ADP off rate of 13–15 s^{-1}, which is what is normally measured for S1 in the absence of strain. Thus what was observed was not acceleration during walking, but an apparent slowing of ADP release during the single encounter of the two-headed molecule. It is likely that the single encounter was in fact a two-headed single encounter, and not simply interaction by one head as assumed by Veigel *et al.* (2002). The data of Veigel *et al.* support this in that the displacement of a two-headed (HMM) single encounter was 25 nm, while that of a one-headed (S1) encounter was 21 nm. If the HMM single (initial) encounter was two-headed, as in the study of Rosenfeld and Sweeney, then its duration at saturating ATP concentrations would be 33 ms (30 s^{-1} ADP off rate from rear head) + 77 ms (13 s^{-1} ADP off rate from the lead head). This is in good agreement with the duration measured by Veigel *et al.* (110 ms versus 107 ms). Thus their data do not support acceleration of ADP release from a rear head during processive movement. Instead they agree with the kinetic data of Rosenfeld and Sweeney which demonstrate acceleration of ADP release from a rear head only occurs during an initial two-headed encounter.

Clearly the geometry of the initial encounter of two-headed myosin V is different from subsequent encounters because both heads begin in pre-powerstroke states. The single event data of Veigel *et al.* suggest that the heads are binding to actin monomers that are ~ 8 nm (~ two actin monomers) apart, and that this geometry allows the lead head to strain the rear head in a manner that accelerates ADP release. When the processive behaviour of a myosin V with a short (4IQ) lever arm was characterized (Purcell *et al.* 2002), the short lever arms constrained the lead head to take 24 nm steps during steady-state movement. Intriguingly, the steady-state ADP release rate from the rear head was accelerated to a similar extent as seen in the initial encounter of wild-type myosin V. One possible explanation for these data is the ADP-releasing isomerization involves a lever arm movement with a significant

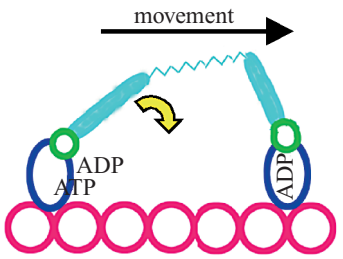

Figure 4. Gating mechanism of myosin V. While the rear head is in a strong-ADP strong-actin binding state, the lead head binds to actin, rapidly releases P_i, undergoes the weak to strong transition, and generates intra-molecular strain. Until the rear head detaches, the lead head cannot undergo sufficient lever arm movement to release ADP. Strain on the rear head cannot accelerate ADP release, except during the initial two-headed encounter (i.e. the first step). Once the rear head releases ADP, ATP rapidly binds and dissociates the rear head. This unbound head moves forward (now in an ADP·P_i state) and binds to actin as the new lead head. The constraint on the former lead head (now rear head) is removed, and the cycle is repeated.

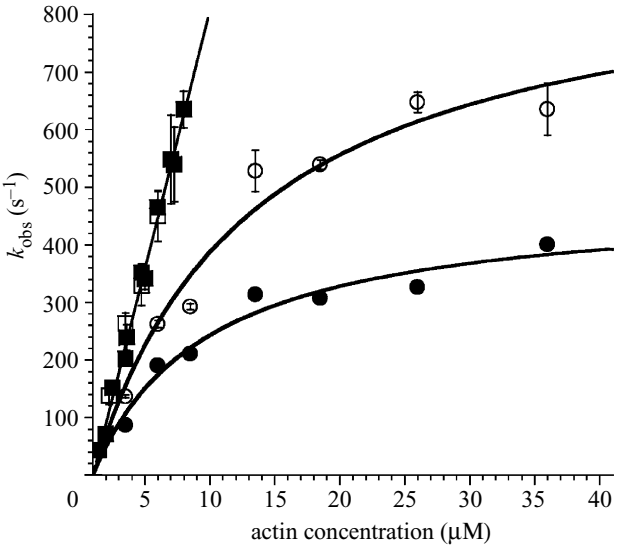

Figure 5. Rates of binding of the MV-1IQ and fast skeletal myosin II (Sk) S1 to pyrene–actin filaments and the dependence on actin concentration. The rates of MV-1IQ and SkS1 binding to pyrene–actin in the absence of nucleotide are plotted as a function of pyrene–actin concentration. Linear fits of the rates (k_{obs}) of MV-1IQ binding to pyrene–actin at 25 °C (filled squares) and 30 °C (open squares). Hyperbolic fits of the rates (k_{obs}) of SkS1 binding to pyrene–actin at 25 °C (filled circles) and 30 °C (open circles).

orthogonal component (relative to the actin filament) that allows off-axis strain to accelerate the isomerization, whereas on-axis strain cannot. Another possibility is that the lever arm compliance is asymmetric, and is greater if pulled forward on-axis than if pulled off-axis.

Ultimately it is unclear as to what is the significance of the acceleration of ADP release from a rear head during an initial actin encounter. Because myosin V traffics through an actin meshwork in cells, it may be a mechanism designed to accelerate ADP release from a rear head if the lead head sidesteps onto a different actin filament. Such a head geometry might allow the lead head to release ADP at an unstrained rate, resulting in simultaneous ADP release from both heads and termination of a processive run. Acceleration of ADP release from the rear head under those conditions could ensure that the run continues.

8. CORRELATION BETWEEN STRUCTURAL AND KINETIC STATES

Understanding the chemo-mechanical coupling in the myosin motor requires assigning structural states to the distinct steps of the actomyosin cycle characterized by kinetic studies. Coupling structural and kinetic studies is not only insightful but it allows the design of mutant myosins to test directly which conformational changes the myosin motor undergoes in the motor cycle. For example, structures of the pre-powerstroke state crystallized when either ATP or ADP·P_i analogues are bound to myosin (Fisher *et al.* 1995; Dominguez *et al.* 1998; Houdusse *et al.* 1999; Bauer *et al.* 2000) show that ATP hydrolysis requires interactions between switch II and the γ-phosphate that result in the closure of the γ-phosphate pocket, preventing P_i release. To avoid steric hindrance, the rigid conformation of switch II in this state must be coupled with precise conformations of both the relay and the SH1 helix that leads to a primed position for the converter and the lever arm, characteristic of the pre-powerstroke conformation of the myosin head (see figures 1 and 2). Site-directed mutagenesis studies have confirmed that this conformation is essential for ATP hydrolysis and is preceded by a lever arm movement (Malnasi-Csizmadia *et al.* 2001). Hydrolysis of ATP in the myosin motor is thus highly correlated with the priming of the lever arm. Trapping of the P_i explains the stability of the pre-powerstroke conformation until actin binding favours an isomerization that allows P_i release. This underlies the low intrinsic ATPase activity of myosin in the absence of actin, and provides the structural basis for the results of Lymn & Taylor (1971).

While the two first structural states identified for myosin provided insight into the mechanism of hydrolysis, and provided support for the lever arm hypothesis (see above), they gave little insight into the force-generating structural changes in myosin that accompanied actin binding. These missing structural states are necessary to understand the details of how rearrangements in the head allow communication from the actin binding site to the nucleotide-binding pocket, which is the essence of chemo–mechanical transduction by the actin–myosin interaction. This is where the unusual kinetics of the processive motor, myosin V, provided a unique opportunity. As shown in figure 5, in the absence of nucleotide, the myosin II motor populates a state (post-rigour) which must undergo a strongly temperature-dependent conformational change upon actin interaction to form the rigour complex. By contrast, myosin V in the absence of nucleotide populates a state that binds to actin in a temperature-independent, diffusion-limited manner (figure 5), suggesting that it is already populating the rigour conformation. Exploiting this fact, a new myosin structural state has been described from crystals of nucleotide-free myosin V. Both kinetic and structural evidence allow us to assert that this new structure reveals details of the rigour structure of myosin, albeit not bound to actin.

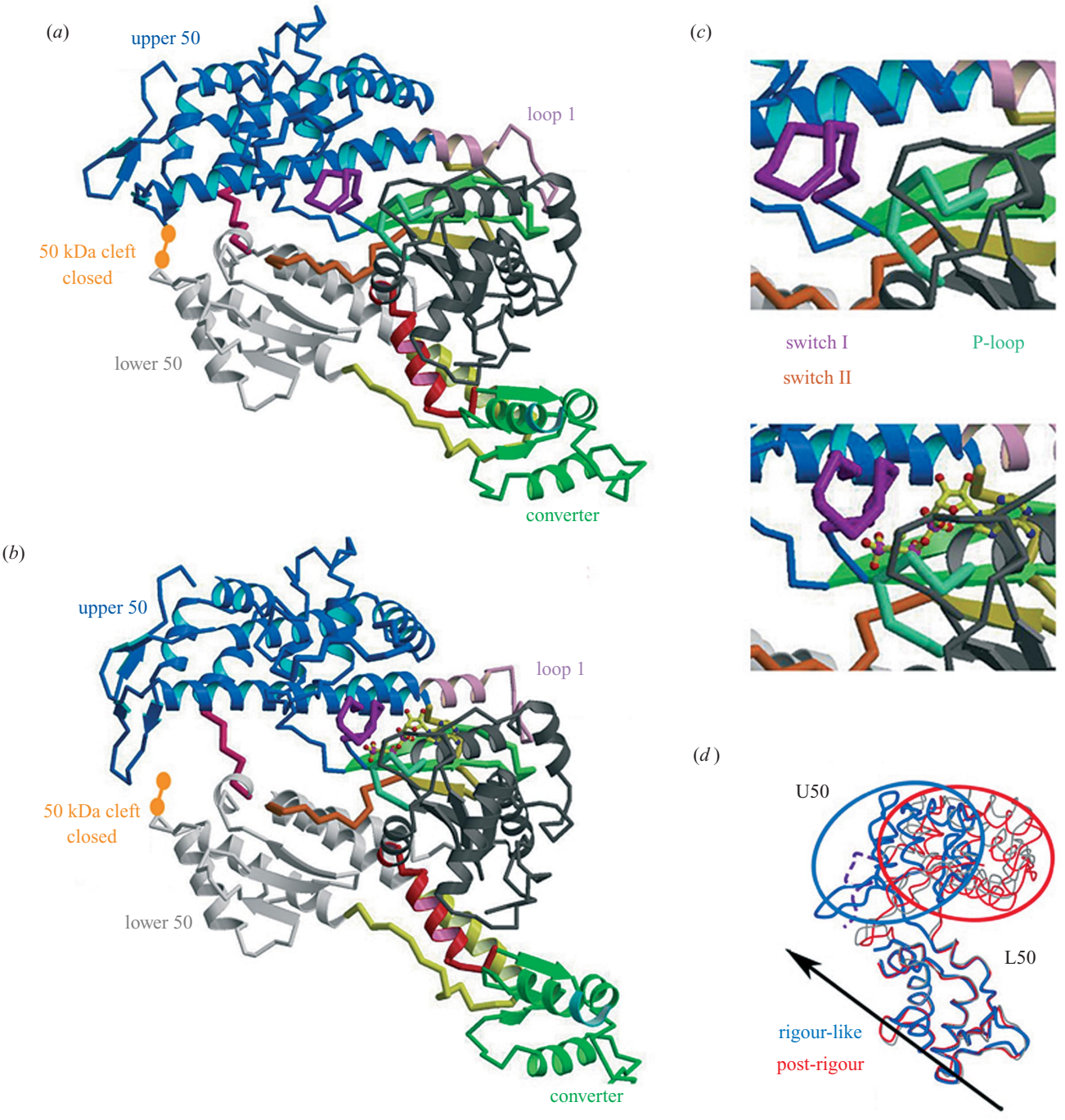

Figure 6. The myosin V rigour-like (nucleotide-free) (*a*) and post-rigour (ATP-state) (*b*) states are shown superimposing the structures on the lower 50 kDa subdomain (grey) so that the degree of cleft closure can easily be compared. Note that the converter (green) is not much affected by the large relative movement of the subdomains in the two structures. (*c*) A closer view of the active sites in (*a*) and (*b*). Note the difference in the position of switch I (purple) upon binding of MgATP. These active site rearrangements trigger re-opening of the 50 kDa cleft and drastically affect the actin interface (*d*) (which is composed of elements from both the lower and upper 50 kDa subdomains).

9. NUCLEOTIDE-FREE MYOSIN V REVEALS A NEW STRUCTURAL STATE

The nucleotide-free myosin V crystals indeed revealed a novel conformation for the myosin head in which all the key features that were predicted to occur in the myosin state with the strongest affinity for F-actin (i.e. rigour state) are realized (Coureux *et al.* 2003). First, as predicted from EM studies, the structure reveals at atomic resolution how the major cleft in the molecule can close without much effect in the lever arm position (see figure 6). In contrast to the post-rigour (ATP−) state for which this cleft is totally open, interactions between the two 50 kDa subdomains allow total closure of this cleft from the actin interface to the nucleotide-binding site in the myosin V structure. Note that the lever arm position found in this structure is consistent with energy transfer measurements (Xiao *et al.*

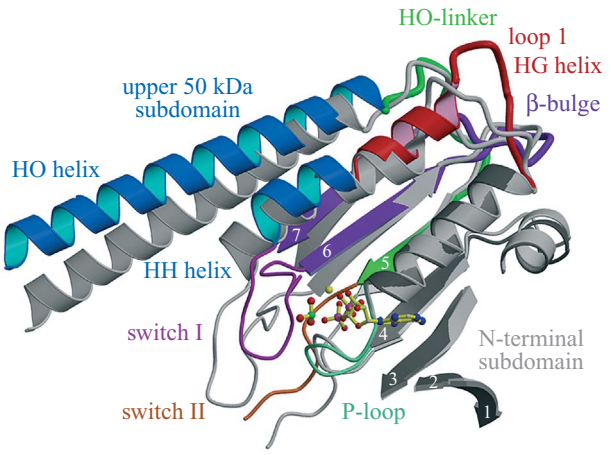

Figure 7. The transducer region found at the boundary between the N-terminal and the upper 50 kDa subdomains is shown for myosin V both in the post-rigour state (coloured) and rigour-like state (grey) after superimposing the structures on the N-terminal subdomain. Note in particular the distortion of the last three strands of the β-sheet and associated loops [loop1 and HG helix (red, residues S184–A198), β-bulge (purple, residues F220–T241) and HO-linker (green, residues L423–D437)]. Switch I (purple, residues A209–R219) follows the rotation of the upper 50 kDa subdomain and is thus found 7 Å away from the nucleotide binding site in the rigour-like structure. Different conformational changes of the P-loop (pale green, residues S162–T170) are necessary to accommodate ATP or ADP in the active site.

2003) that do not report significant lever arm swing (no reversal in the power-stroke) when ATP binding to actomyosin induces dissociation. The closure of the cleft brings closer together different elements of the actin binding interface consistent with a major increase in the affinity for the filament for this state compared with the post-rigour and pre-powerstroke states. Finally, major rearrangements and new interactions between the nucleotide-binding elements (P-loop, switch I and switch II) found in the myosin V structure are consistent with the weak affinity of the rigour state for the nucleotide (see figure 6). In revealing unexpected rearrangements in the molecule, this new structure demonstrates for the first time, to our knowledge, the structural basis of the coupling between the binding and release of actin and nucleotide, and the strong inverse linkage that has remained enigmatic.

While closure of the cleft had been predicted, the structural changes in the molecule that facilitated cleft closure were not. The key structural rearrangement is an unexpected distortion of the seven-stranded beta sheet that lies at the boundary of the N-terminal and upper 50 kDa subdomains, where lies the nucleotide-binding site. This distortion is accommodated by associated linker and loop elements we have collectively named the transducer (diagrammed in figure 7). A second crystal form of myosin V with ATP-analogues bound has revealed at 2.0 Å resolution the exact rearrangements that occur on the motor upon ATP binding (Coureux *et al.* 2004). Structural changes of the transducer play a key role to allow large relative rotation of the subdomains, which are critical to coordinate changes in the actin-binding interface with rearrangements in the nucleotide-binding site.

To ascertain the nature of ADP binding to the A.M.D^{W} state, myosin V nucleotide-free crystals were soaked in 10 mM MgADP. Interestingly, the ADP is coordinated exclusively by the P-loop, without Mg^{2+} and without any contributions from switch I or switch II. There are subtle rearrangements of the nucleotide binding elements, especially the P-loop, compared with the rigour structure. Otherwise the structure is not different from the nucleotide-free state. This supports the contention that the A.M.D^{W} state is essentially a rigour conformation, thus implying that the powerstroke terminates with the lever arm in the rigour position. The fact that the Mg^{2+} ion is not bound in this structure suggests that coordination by switch I residues is critical for the Mg^{2+} affinity. This structure has important physiological implications, in that it suggests that Mg^{2+} is released before ADP from actomyosin (figure 3). Moreover, this structure is the first one, to our knowledge, to show how P-loop rearrangements could differ when ADP or ATP needs to be accommodated in the active site.

10. MISSING STRUCTURAL STATES

While the high-resolution structures currently known have elucidated the ATP binding and hydrolysis steps, we have little insight into the structural intermediates between the initial weak interaction of the pre-powerstroke state with actin, and the release of inorganic P_i and formation of strong actin binding. Thus our high-resolution view of the actomyosin ATPase cycle is currently as summarized in figure 8.

As summarized in figure 3, there is kinetic evidence for the existence of two additional states that have not been visualized at high resolution (Houdusse & Sweeney 2001). Specifically, there must be formation of an actin·myosin·ADP state (A.M^{SH}.D^{S} state) from the pre-powerstroke state to provide an escape route for the inorganic P_i. In many myosins such as myosin V, a strong actin-binding, strong ADP-binding state (A.M.D^{S} state) precedes the rigour state (figure 3), which must be followed by a weak ADP binding state (A.M.D^{W} state), that gives rise to rigour upon ADP dissociation (Rosenfeld *et al.* 2000).

The new myosin V structures have changed our views of the possible structural changes that may occur when myosin binds to actin and generates force and movement. Indeed, the unexpected rearrangements found in these structures not only demonstrate how actin favours nucleotide exchange and how MgATP binding reduces the myosin affinity for actin. They give novel insights about how different types of distortion in the transducer and variations in the P-loop conformation can be exploited to achieve the earlier product release steps.

11. SLEEP STATE IS NOT EQUIVALENT TO THE POST-RIGOUR STATE

The existence of a specific state for P_i release came first from the kinetic studies of Sleep & Hutton (1980), hence the myosin designation, M^{SH}. When the first myosin structures appeared, it was evident that the P_i would be trapped in the pre-powerstroke structure following hydrolysis, but that an escape route, referred to as a 'back door' (Yount *et al.* 1995), existed for the P_i in the post-rigour structure. This caused us to speculate that actin might cause the motor to transiently adopt a post-rigour confor-

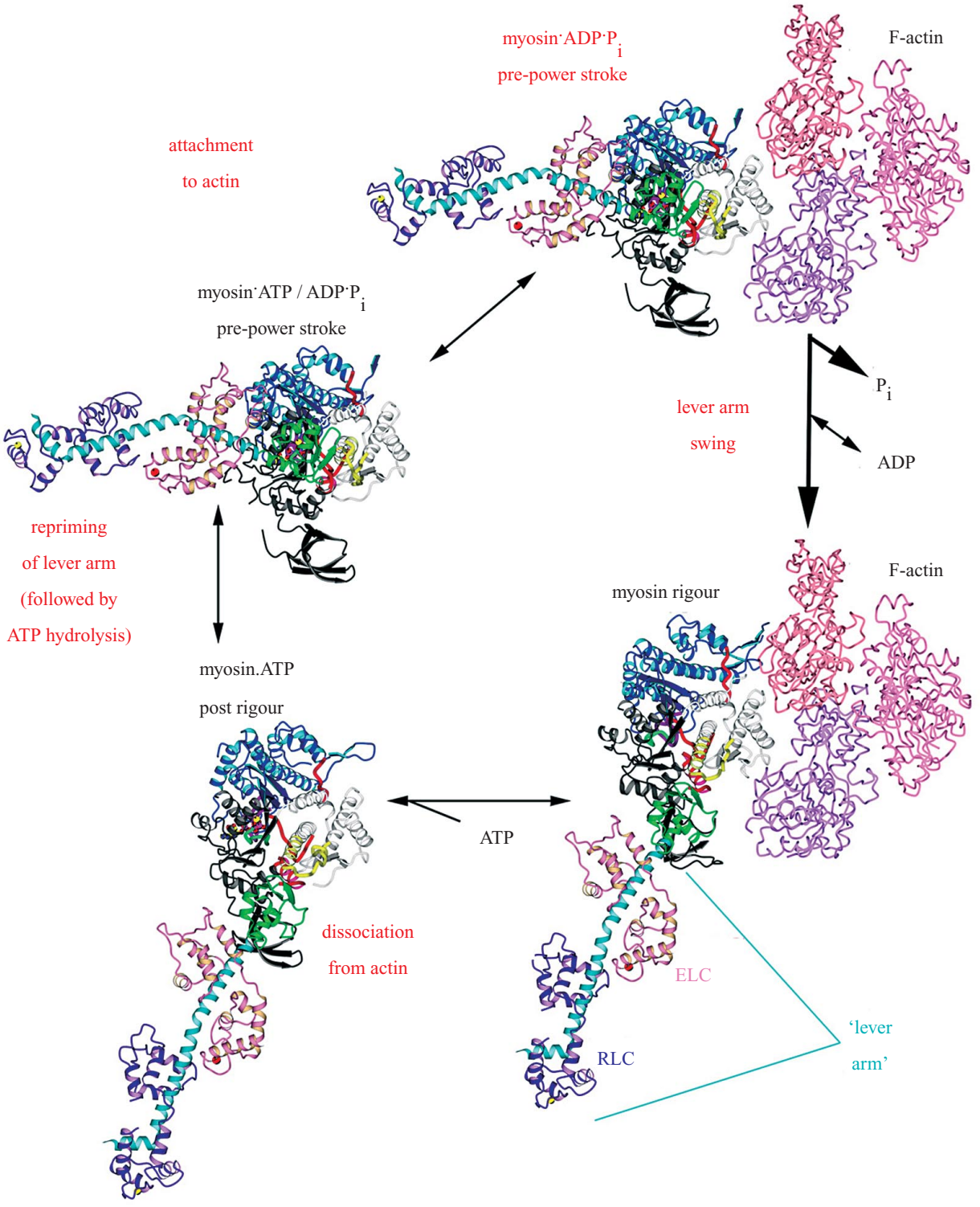

Figure 8. High-resolution structures of myosin placed within the actin-activated ATPase cycle. The post-rigour and pre-powerstroke states pictured are from scallop myosin II. The rigour conformation is the motor from the chicken myosin V rigour-like structure to which the scallop myosin II lever arm has been modelled onto the converter.

mation so as to release P_i from the pre-powerstroke state (Houdusse & Sweeney 2001). However, recent molecular dynamics modelling suggests that there is not adequate room for P_i escape in the post-rigour state (Lawson *et al.* 2004). Additionally there is now evidence for the existence of a state different from the post-rigour state for myosin V from which P_i is released. A rapid mant-nucleotide fluorescence change was detected by Rosenfeld & Sweeney (2004), which corresponded to the rate of P_i release. No change in mant-ATP signal is associated with an isomerization between the post-rigour and pre-powerstroke states. Based on the published *Dictyostelium* myosin II structure with mant·ADP bound (Bauer *et al.* 1997), our interpretation of this is that the structural transition that allows release of P_i results in a change in the environment of the mant because of a rearrangement involving switch I. This is

the first evidence that we have to suggest a change in switch I to create an exit route for P_i release, even though there is maintenance of strong binding of the MgADP. A second change in mant fluorescence is seen upon ADP release, probably a result of a complete removal of switch I, as seen in the rigour structure. Thus the picture that emerges is that switch I must reposition in some manner to create an exit route for the P_i, but still maintain coordination of nucleotide.

It also is clear from the same study of Rosenfeld & Sweeney (2004) that the conformational change that allows P_i release precedes the conformational change that causes pyrene–actin quenching (strong binding). Thus the Sleep (M^{SH}) state undoubtedly has an altered actin interface compared with the pre-powerstroke state (to communicate with the nucleotide pocket), and probably an actin-binding affinity that is intermediate between a 'weak' and 'strong' state. The recent structures of myosin V (Coureux *et al.* 2003, 2004) suggest that the actin-bound conformations of myosin will be characterized by beta-sheet distortions that do not occur in the post-rigour and pre-powerstroke states. Thus the structural details of the Sleep state are still unclear, but probably will involve a different type of beta-sheet distortion than seen in rigour to accommodate both actin and nucleotide binding.

12. THE STRONG ADENOSINE DIPHOSPHATE ACTIN BOUND STATE

The next defined state in the actomyosin ATPase cycle (figure 3) has been detected kinetically and imaged at low resolution with cryoEM. It is the state that binds strongly to actin (following the weak to strong transition that quenches pyrene–actin) and maintains a high affinity for MgADP. It was first detected by a lever arm 'swing' upon ADP release in smooth MII, using cryoEM (Whitaker *et al.* 1995), and is present in most myosin isoforms. In essence there is an equilibrium between a strong actin-strong ADP state ($A.M.D^S$) and a state that binds actin strongly, but ADP weakly ($A.M.D^W$), that is probably equivalent to the rigour state (see also Nyitrai & Geeves 2004). The apparent rate of ADP dissociation is determined primarily by the rate of the isomerization between these two states, because ADP dissociation is rapid from the $A.M.D^W$ state (Rosenfeld *et al.* 2000). Thus the difference in ADP dissociation rates between smooth MII and NMIIB is determined by the different rates and equilibria associated with the isomerization. Because the isomerization involves a lever arm swing, it creates a strain dependent step. For smooth myosin II the equilibrium is poised to slow ADP release under load, whereas in the case of NMIIB, ADP is released very slowly unless another myosin pulls (towards the rigour position) on the lever arm. As already discussed above, in the case of myosin V, a lead head is prevented from undergoing this isomerization until the rear head detaches.

As in the case of the Sleep (M^{SH}) state, the structural details of the motor domain in the strong ADP state ($A.M.D^S$) are unknown. Again we would speculate that beta-sheet distortions distinct from those seen in rigour and those likely to be found in the Sleep state may allow the formation of a strong actin binding interface and maintain high-affinity nucleotide binding. Structural variations among isoforms probably dictate how easily these distortions are accommodated. On one extreme is non-muscle myosin IIB, which almost exclusively populates the strong ADP state ($A.M.D^S$) in the absence of strain, resulting in a MgADP affinity that is unaltered by actin binding (Rosenfeld *et al.* 2003). At the other extreme are skeletal and *Dictyostelium* myosin IIs, which cannot populate the strong ADP state in the absence of strain and thus have very low MgADP affinities when bound to actin (Gollub *et al.* 1996; Rosenfeld *et al.* 2000; Volkman *et al.* 2003).

13. CONCLUSIONS

The kinetic and structural states of myosin V as well as the mechanisms of its movement are understood at a level that surpasses that for all other myosins. At the same time the findings on myosin V are providing greater insights into how myosins work in general, and into the mechanism of muscle contraction. What is still missing are not only the structural details of the states involved in the force generating steps on actin, but also the effects of imposed strain on all of the static motor domain structures. This point has recently been highlighted by EM images of two-headed molecules of myosin V with the heads bound 36 nm apart on an actin filament (Walker *et al.* 2000; Burgess *et al.* 2002). The lever arm of the lead head is in a position similar to the pre-powerstroke state even though, based on kinetic studies, the state of the head is likely to be either strong ADP or rigour. As we noted in an earlier review, understanding where the 'springs' are within the motor that can accommodate such strain and still allow strong binding to actin is as important as understanding the details of the initial actin-bound states in which force is generated. Thus the final solution of how muscle works that began with the monumental papers by the Huxleys and their colleagues in 1954, awaits the delineation of the 'missing structures and hidden springs'.

This work was supported by grants from the National Institutes of Health (H.L.S.) and the CNRS (A.H.).

REFERENCES

Batters, C., Wallace, M. I., Coluccio, L. M. & Molloy, J. E. 2004 A model of stereocilia adaptation based on single molecule mechanical studies of myosin-I. *Phil. Trans. R. Soc. B* **359**, 1895–1905. (doi:10.1098/rstb.2004.1559)

Bauer, C. B., Kuhlman, P. A., Bagshaw, C. R. & Rayment, I. 1997 X-ray crystal structure and solution fluorescence characterization of Mg.2'(3')-O-(N-methylanthraniloyl) nucleotides bound to the *Dictyostelium discoideum* myosin motor domain. *J. Mol. Biol.* **274**, 394–407.

Bauer, C. B., Holden, H. M., Thoden, J. B., Smith, R. & Rayment, I. 2000 X-ray structures of the apo and MgATP-bound states of *Dictyostelium discoideum* myosin motor domain. *J. Biol. Chem.* **275**, 38 494–38 499.

Burgess, S., Walker, M., Wang, F., Sellers, J. R., White, H. D., Knight, P. J. & Trinick, J. 2002 The prepower stroke conformation of myosin V. *J. Cell Biol.* **159**, 983–991.

Cain, D. F. & Davies, R. E. 1962 Breakdown of adenosine triphosphate during a single contraction of working muscle. *Biochem. Biophys. Res. Commun.* **8**, 361–366.

Carragher, B. O., Cheng, N., Wang, Z. Y., Korn, E. D., Reilein, A., Belnap, D. M., Hammer 3rd, J. A. & Steven, A. C. 1998 Structural invariance of constitutively active and inactive mutants of acanthamoeba myosin IC bound to F-actin in the rigor and ADP-bound states. *Proc. Natl Acad. Sci. USA* **95**, 15 206–15 211.

Coureux, P.-D., Wells, A. L., Ménétrey, J., Yengo, C. M., Morris, C. A., Sweeney, H. L. & Houdusse, A. 2003 A structural state of the myosin V motor without bound nucleotide. *Nature* **425**, 419–423.

Coureux, P.-D., Sweeney, H. L. & Houdusse, A. 2004 Three myosin V structures delineate essential features of chemo-mechanical transduction. *EMBO J.* **23**, 4527–4537.

Cremo, C. R. & Geeves, M. A. 1998 Interaction of actin and ADP with the head domain of smooth muscle myosin: implications for strain-dependent ADP release in smooth muscle. *Biochemistry* **37**, 1969–1978.

Dantzig, J. A., Goldman, Y. E., Millar, N. C., Lacktis, J. & Homsher, E. 1992 Reversal of the cross-bridge force-generating transition by photogeneration of phosphate in rabbit psoas muscle fibres. *J. Physiol.* **451**, 247–278.

De La Cruz, E. M., Wells, A. L., Safer, D., Ostap, E. M. & Sweeney, H. L. 1999 The kinetic mechanism of myosin V. *Proc. Natl Acad. Sci. USA* **96**, 13 726–13 731.

Dominguez, R., Freyzon, Y., Trybus, K. M. & Cohen, C. 1998 Crystal structure of a vertebrate smooth muscle myosin motor domain and its complex with the essential light chain: visualization of the pre-power stroke state. *Cell* **94**, 559–571.

Fisher, A. J., Smith, C. A., Thoden, J. B., Smith, R., Sutoh, K., Holden, H. M. & Rayment, I. 1995 X-ray structures of the myosin motor domain of *Dictyostelium discoideum* complexed with MgADP.BeFx and MgADP.AlF^{4-}. *Biochemistry* **34**, 8960–8972.

Forkey, J. N., Quinlan, M. E., Shaw, M. A., Corrie, J. E. & Goldman, Y. E. 2003 Three-dimensional structural dynamics of myosin V by single-molecule fluorescence polarization. *Nature* **422**, 399–404.

Geeves, M. A. & Holmes, K. C. 1999 Structural mechanism of muscle contraction. *A. Rev. Biochem.* **68**, 687–728.

Gollub, J., Cremo, C. R. & Cooke, R. 1996 ADP release produces a rotation of the neck region of smooth myosin but not skeletal myosin. *Nature Struct. Biol.* **3**, 796–802.

Holmes, K. C. 1996 Muscle proteins: their actions and interactions. *Curr. Opin. Struct. Biol.* **6**, 781–789.

Holmes, K. C., Popp, D., Gebhard, W. & Kabsch, W. 1990 Atomic model of the actin filament. *Nature* **347**, 44–49.

Holmes, K. C., Angert, I., Kull, F. J., Jahn, W. & Schröder, R. R. 2003 Electron cryo-microscopy shows how strong binding of myosin to actin releases nucleotide. *Nature* **425**, 423–427.

Holmes, K. C., Schröder, R. R. , Eschenburg, S., Sweeney, H. L. & Houdusse, A. 2004 The structure of the rigor complex and its implications for the power stroke. *Phil. Trans. R. Soc. B* **359**, 1819–1828. (doi:10.1098/rstb.2004.1566)

Houdusse, A. & Sweeney, H. L. 2001 Myosin motors: missing structures and hidden springs. *Curr. Opin. Struct. Biol.* **11**, 182–194.

Houdusse, A., Kalabokis, V. N., Himmel, D., Szent-Gyorgyi, A. G. & Cohen, C. 1999 Atomic structure of scallop myosin subfragment S1 complexed with MgADP: a novel conformation of the myosin head. *Cell* **97**, 459–470.

Houdusse, A., Szent-Györgyi, A. G. & Cohen, C. 2000 Three conformational states of scallop myosin S1. *Proc. Natl Acad. Sci. USA* **97**, 11 238–11 243.

Huxley, A. F. & Niedergerke, R. 1954 Structural changes in muscle during contraction; interference microscopy of living muscle fibres. *Nature* **173**, 971–973.

Huxley, A. F. & Simmons, R. M. 1971 Proposed mechanism of force generation in striated muscle. *Nature* **233**, 533–538.

Huxley, H. E. 1957 The double array of filaments in cross-striated muscle. *J. Biophys. Biochem. Cytol.* **3**, 631–648.

Huxley, H. E. 1969 The mechanism of muscular contraction. *Science* **164**, 1356–1359.

Huxley, H. E. & Hanson, J. 1954 Changes in the cross-striations of muscle during contraction and stretch and their structural interpretation. *Nature* **173**, 973–976.

Jontes, J. D., Wilson-Kubalek, E. M. & Milligan, R. A. 1995 A 32 degree tail swing in brush border myosin I on ADP release. *Nature* **378**, 751–753.

Jontes, J. D., Ostap, E. M., Pollard, T. D. & Milligan, R. A. 1998 Three-dimensional structure of *Acanthamoeba castellanii* myosin-IB (MIB) determined by cryoelectron microscopy of decorated actin filaments. *J. Cell Biol.* **141**, 155–162.

Kabsch, W., Mannherz, H. G., Suck, D., Pai, E. F. & Holmes, K. C. 1990 Atomic structure of the actin:DNase I complex. *Nature* **347**, 37–44.

Kollmar, M., Durrwang, U., Kliche, W., Manstein, D. J. & Kull, F. J. 2002 Crystal structure of the motor domain of a class-I myosin. *EMBO J.* **21**, 2517–2525.

Lawson, J. D., Pate, E., Rayment, I. & Yount, R. G. 2004 Molecular dynamics analysis of structural factors influencing back door P_i release in myosin. *Biophys. J.* **86**, 3794–3803.

Lorenz, M., Popp, D. & Holmes, K. C. 1993 Refinement of the F-actin model against X-ray fiber diffraction data by the use of a directed mutation algorithm. *J. Mol. Biol.* **234**, 826–836.

Lymn, R. W. & Taylor, E. W. 1971 Mechanism of adenosine triphosphate hydrolysis by actomyosin. *Biochemistry* **10**, 4617–4624.

Malnasi-Csizmadia, A., Pearson, D. S., Kovacs, M., Woolley, R. J., Geeves, M. A. & Bagshaw, C. R. 2001 Kinetic resolution of a conformational transition and the ATP hydrolysis step using relaxation methods with a *Dictyostelium* myosin II mutant containing a single tryptophan residue. *Biochemistry* **40**, 12 727–12 737.

Manstein, D. J. 2004 Molecular engineering of myosin. *Phil. Trans. R. Soc. B* **359**, 1907–1912. (doi:10.1098/rstb.2004.1565)

Mehta, A. D., Rock, R. S., Rief, M., Spudich, J. A., Mooseker, M. S. & Cheney, R. E. 1999 Myosin V is a processive actin-based motor. *Nature* **400**, 590–593.

Moore, J. R., Krementsova, E. B., Trybus, K. M. & Warshaw, D. M. 2004 Does the myosin V neck region act as a lever? *J. Muscle Res. Cell Motil.* **25**, 29–35.

Nyitrai, M. & Geeves, M. A. 2004 ADP and strain sensitivity in myosin motors. *Phil. Trans. R. Soc. B* **359**, 1867–1877. (doi:10.1098/rstb.2004.1560)

Otterbein, L. R., Graceffa, P. & Dominguez, R. 2001 The crystal structure of uncomplexed actin in the ADP state. *Science* **293**, 708–711.

Pollard, T. D. & Korn, E. D. 1973 Acanthamoeba myosin. I. Isolation from *Acanthamoeba castellanii* of an enzyme similar to muscle myosin. *J. Biol. Chem.* **248**, 4682–4690.

Purcell, T. J., Morris, C., Spudich, J. A. & Sweeney, H. L. 2002 Role of the lever arm in the processive stepping of myosin V. *Proc. Natl Acad. Sci. USA* **99**, 14 159–14 164.

Rayment, I., Rypniewski, W. R., Schmidt-Bäde, K., Smith, R., Tomchick, D. R., Benning, M. M., Winkelmann, D. A., Wesenberg, G. & Holden, H. M. 1993*a* Three-dimensional structure of myosin subfragment-1: a molecular motor. *Science* **261**, 50–58.

Rayment, I., Holden, H. M., Whitaker, M., Yohn, C. B., Lorenz, M., Holmes, K. C. & Milligan, R. A. 1993*b* Structure of the actin-myosin complex and its implications for muscle contraction. *Science* **261**, 58–61.

Rosenfeld, S. S. & Sweeney, H. L. 2004 A model for myosin V processivity. *J. Biol. Chem.* **279**, 40 100–40 111.

Rosenfeld, S. S., Xing, J., Whithaker, M., Cheung, H. C., Brown, F., Wells, A., Milligan, R. A. & Sweeney, H. L. 2000 Kinetic and spectroscopic evidence for three actomyosin:ADP states in smooth muscle. *J. Biol. Chem.* **275**, 25 418–25 426.

Rosenfeld, S. S., Xing, J., Chen, L. Q. & Sweeney, H. L. 2003 Myosin IIb is unconventionally conventional. *J. Biol. Chem.* **278**, 27 449–27 455.

Sakamoto, T., Wang, F., Schmitz, S., Xu, Y., Xu, Q., Molloy, J. E., Veigel, C. & Sellers, J. R. 2003 Neck length and processivity of myosin V. *J. Biol. Chem.* **278**, 29 201–29 207.

Schröder, R. R., Manstein, D. J., Jahn, W., Holden, H., Rayment, I., Holmes, K. C. & Spudich, J. A. 1993 Three-dimensional atomic model of F-actin decorated with *Dictyostelium* myosin S1. *Nature* **364**, 171–174.

Sleep, J. A. & Hutton, R. L. 1980 Exchange between inorganic phosphate and adenosine 5′-triphosphate in the medium by actomyosin subfragment 1. *Biochemistry* **19**, 1276–1283.

Uyeda, T. Q., Abramson, P. D. & Spudich, J. A. 1996 The neck region of the myosin motor domain acts as a lever arm to generate movement. *Proc. Natl Acad. Sci. USA* **93**, 4459–4464.

Veigel, C., Wang, F., Bartoo, M. L., Sellers, J. R. & Molloy, J. E. 2002 The gated gait of the processive molecular motor, myosin V. *Nature Cell Biol.* **4**, 59–65.

Volkman, N., Hanein, D., Ouyang, G., Trybus, K. M., DeRosier, D. J. & Lowey, S. 2000 Evidence for cleft closure in actomyosin upon ADP release. *Nature Struct. Biol.* **7**, 1147–1155.

Volkman, N., Ouyang, G., Trybus, K. M., DeRosier, D. J., Lowey, S. & Hanein, D. 2003 Myosin isoforms show unique conformations in the actin-bound state. *Proc. Natl Acad. Sci. USA* **100**, 3227–3232.

Walker, M. L., Burgess, S. A., Sellers, J. R., Wang, F., Hammer 3rd, J. A., Trinick, J. & Knight, P. J. 2000 Two-headed binding of a processive myosin to F-actin. *Nature* **405**, 804–807.

Warshaw, D. M., Guilford, W. H., Freyzon, Y., Krementsova, E., Palmiter, K. A., Tyska, M. J., Baker, J. E. & Trybus, K. M. 2000 The light chain binding domain of expressed smooth muscle heavy meromyosin acts as a mechanical lever. *J. Biol. Chem.* **275**, 37 167–37 172.

Whitaker, M., Wilson-Kubalek, E. M., Smith, J. E., Faust, L., Milligan, R. A. & Sweeney, H. L. 1995 A 35 Å movement of smooth muscle myosin on ADP release. *Nature* **378**, 748–751.

Xiao, M., Reifenberger, J. G., Wells, A. L., Baldacchino, C., Chen, L. Q., Ge, P., Sweeney, H. L. & Selvin, P. R. 2003 An actin-dependent conformational change in myosin. *Nature Struct. Biol.* **10**, 402–408.

Yengo, C. M., Chrin, L., Rovner, A. S. & Berger, C. L. 1999 Intrinsic tryptophan fluorescence identifies specific conformational changes at the actomyosin interface upon actin binding and ADP release. *Biochemistry* **38**, 14 515–14 523.

Yildiz, A., Forkey, J. N., McKinney, S. A., Ha, T., Goldman, Y. E. & Selvin, P. R. 2003 Myosin V walks hand-over-hand: single fluorophore imaging with 1.5 nm localization. *Science* **300**, 2061–2065.

Yount, R. G., Lawson, D. & Rayment, I. 1995 Is myosin a 'back door' enzyme? *Biophys. J.* **68**(Suppl. 4), 44S–47S.

GLOSSARY

A.M.D: actomyosin complex with ADP bound in the myosin active site
ADP: adenosine diphosphate
ATP: adenosine triphosphate
cryoEM: cryo-electron microscopy
D: ADP
EM: electron microscopy
HMM: heavy mero-myosin
IQ: IQ motif, a light chain binding motif
M**: high fluorescence myosin state
M*: low fluorescence myosin state
mant-ADP: the fluorescent substrate analogue methyl-anthraniloyl ADP
MgADP: Mg^{2+}·ADP
NMIIB: non-muscle myosin IIB
P: inorganic phosphate P_i
S1: subfragment 1
SH1: the most reactive thiol group of the motor domain.